

# The HIPASS catalogue: $\Omega_{\text{HI}}$ and environmental effects on the H I mass function of galaxies

M. A. Zwaan,<sup>1</sup> M. J. Meyer,<sup>2</sup> L. Staveley-Smith<sup>3</sup> and R. L. Webster<sup>4</sup>

<sup>1</sup> European Southern Observatory, Karl-Schwarzschild-Str. 2, 85748 Garching b. München, Germany.

<sup>2</sup> Space Telescope Science Institute, 3700 San Martin Drive, Baltimore MD 21218, USA.

<sup>3</sup> Australia Telescope National Facility, CSIRO, P.O. Box 76, Epping, NSW 1710, Australia.

<sup>4</sup> School of Physics, University of Melbourne, VIC 3010, Australia.

Accepted 2005 February 9; Received 2005 February 1; in original form 2004 November 29

## ABSTRACT

We use the catalogue of 4315 extragalactic H I 21-cm emission line detections from HIPASS to calculate the most accurate measurement of the H I mass function (HIMF) of galaxies to date. The completeness of the HIPASS sample is well characterised, which enables an accurate calculation of space densities. The HIMF is fitted with a Schechter function with parameters:  $\alpha = -1.37 \pm 0.03 \pm 0.05$ ,  $\log(M_{\text{HI}}^*/M_{\odot}) = 9.80 \pm 0.03 \pm 0.03 h_{75}^{-2}$ , and  $\theta^* = (6.0 \pm 0.8 \pm 0.6) \times 10^{-3} h_{75}^3 \text{ Mpc}^{-3}$  (random and systematic uncertainties at 68% CL), in good agreement with calculations based on the HIPASS Bright Galaxy Catalogue, which is a complete, but smaller, sub-sample of galaxies. The cosmological mass density of H I in the local universe is found to be  $\Omega_{\text{HI}} = (3.5 \pm 0.4 \pm 0.4) \times 10^{-4} h_{75}^{-1}$ . This large homogeneous sample allows us to test whether the shape of the HIMF depends on local galaxy density. We find tentative evidence for environmental effects in the sense that the HIMF becomes *steeper* toward *higher* density regions, ranging from  $\alpha \approx -1.2$  in the lowest density environments to  $\alpha \approx -1.5$  in the highest density environments probed by this blind H I survey. This effect appears stronger when densities are measured on larger scales.

**Key words:** methods: observational – methods: statistical – surveys – radio lines: galaxies – galaxies: statistics

## 1 INTRODUCTION

The concept of the H I mass function (HIMF) of galaxies was introduced by Briggs (1990) as a diagnostic tool for assessing the completeness of optical galaxy catalogues against 21-cm H I surveys. In that paper the then available luminosity functions and an adopted relation between gas richness  $M_{\text{HI}}/L$  and luminosity  $L$  were used to make the first preliminary HIMF calculations. Since then much effort has been put into improving the calculations, mostly based on blind 21-cm H I surveys because these – by definition – have no bias against optically faint, gas-bearing galaxies (Zwaan et al. 1997; Kraan-Korteweg et al. 1999; Schneider, Spitzak, & Rosenberg 1998; Rosenberg & Schneider 2002; Zwaan et al. 2003, hereafter Z03). The accuracy with which the HIMF can be evaluated has improved significantly since Briggs' (1990) original calculation, but interestingly, the shape and normalisation of the field galaxy HIMF have not changed much. This is illustrative of the fact that the galaxy population seen in 21-cm emission is essentially the same to that seen in the optical or IR wavelength, but obviously weighted toward the more gas

rich galaxies, and hence to the late morphological types. Two interesting conclusions can be drawn from the results of the 21-cm surveys: 1) There does not seem to be a large population of low surface brightness galaxies that is overlooked in optical surveys (cf., Disney 1976). This conclusion is also reached by deep large area optical surveys such as the Sloan Digital Sky Survey (SDSS, Blanton et al. 2001) and the Two degree Field Galaxy Redshift Survey (2dFGRS Cross & Driver 2002), as well as by the Millennium Galaxy Survey (MGC, Driver et al. 2005). 2) There appear to be no – or at least very few – isolated self-gravitating H I clouds without stars, or “dark galaxies”. These results are very important for our understanding of the galaxy population of the local universe.

Once an accurate HIMF has been measured, it can be used to evaluate the total mass density of neutral hydrogen atoms in the local Universe,  $\Omega_{\text{HI}}(z = 0)$ . At higher redshifts, the highest column density QSO absorption line systems are used to measure  $\Omega_{\text{HI}}$ , and these measurements have shown that the comoving neutral gas density at  $z = 2 - 5$  is approximately a tenth of a percent of the present critical density of the Universe and about half of the mass density in stars at the present epoch (e.g., Storrie-Lombardi & Wolfe 2000; Péroux et al. 2003). For a good understanding of the evolution of

\* email:mzwaan@eso.org

the Universe's H I content, the measurement of a local benchmark is obviously very important.

One aspect of the HIMF, its dependence on environment, has not been studied in detail because samples of H I-selected galaxies were not large enough to address this issue. Recently, there has been much interest in the environmental effects on star formation rate (Lewis et al. 2002; Balogh et al. 2004), the luminosity function (Croton et al. 2004), and luminosity, surface brightness and colour (Hogg et al. 2003). Since the H I properties of galaxies are intimately tied to the process of star formation, gaining knowledge on the environmental effects on H I properties will help understanding the above mentioned results. Two previous studies discussed environmental effects on the HIMF: Rosenberg & Schneider (2002) compared the field HIMF with that in a cluster region and Springob, Haynes & Giovanelli (2004) studied the HIMF of optically selected galaxies. In this *Letter* we will present for the first time a study of the environmental effects on the HIMF for a large sample of H I-selected galaxies.

The measurement of an accurate HIMF was one of the primary science drivers for the H I Parkes All Sky Survey (HIPASS). This survey, which blindly searched the whole southern sky for 21-cm H I line emission, has now been completed and the catalogue of 4315 extragalactic H I signals has been released to the public (Meyer et al. 2004; Zwaan et al. 2004). A HIMF based on the 1000 HIPASS galaxies with the highest H I peak fluxes (Koribalski et al. 2004), was published in Z03. This *Letter* presents the state-of-the-art HIMF using the full HIPASS catalogue. The velocity coverage of HIPASS is  $-1200$  to  $12,700$  km s $^{-1}$  and the typical noise level is  $13$  mJy beam $^{-1}$ . See Meyer et al. (2004) for more details on the HIPASS catalogue. Throughout this *Letter* we use  $H_0 = 75$  km s $^{-1}$  Mpc $^{-1}$  to calculate distance dependent quantities.

## 2 CALCULATING THE HIMF

In Z03 we derived a bivariate stepwise maximum likelihood (2DSWML) technique, which solves for the space density of objects as a function of H I mass ( $M_{\text{HI}}$ ) and velocity width ( $W$ ) simultaneously. For bins  $j$  in  $\log M_{\text{HI}}$  and bins  $k$  in  $\log W$  the space density  $\theta_{jk}$  can be determined iteratively by evaluating the maximum likelihood solution derived by Efstathiou, Ellis, & Peterson (1988):

$$\theta_{jk} = n_{jk} \left( \sum_{i=1}^{N_g} H_{ijk}/\Theta_i \right)^{-1}, \quad (1)$$

where  $n_{jk}$  is the number of galaxies in each bin,  $H_{ijk}$  is a function that causes the summation to only go over the galaxies that are within the volume accessible to sources in bin  $jk$ . The denominator  $\Theta_i$  is the integral over the bivariate H I mass function defined as

$$\Theta_i = \int_{M_{\text{HI}}=0}^{\infty} \int_{W=0}^{\infty} C(S', S'_{\text{int}}) \theta(M_{\text{HI}}, W) dM_{\text{HI}} dW, \quad (2)$$

where  $C$  is a function that makes the integral go over the mass and velocity range that source  $i$  could have and still be detectable at its distance  $D_i$ , and

$$S' = S^i (M_{\text{HI}}/M_{\text{HI}}^i) (W^i/W), \quad (3)$$

$$S'_{\text{int}} = S^i_{\text{int}} M_{\text{HI}}/M_{\text{HI}}^i \quad (4)$$

are the effective peak flux and integrated flux of source  $i$  if its H I mass would change from  $M_{\text{HI}}^i$  to  $M_{\text{HI}}$  and its velocity width would change from  $W^i$  to  $W$ .

In Z03 we specifically designed this method for a peak-flux-limited sample. However, the equations given above are generally applicable for samples constructed using different selection criteria. The function  $C$ , which can be interpreted as a completeness function, is defined by the selection criteria of the sample. For example, by setting  $C = 0$  for  $S'$  smaller than the peak-flux-limit and  $C = 1$  otherwise, the method is again equivalent to the peak-flux-limited case in Z03.

It can be easily seen that the part between the parentheses in equation 1 is essentially the effective volume available to sources in bin  $jk$ . The important modification that we make here to the SWML method, is that instead of evaluating the summation per bin  $jk$ , we calculate the effective volume for each galaxy individually by iteration:

$$V_{\text{eff}}^i = \sum_{j=1}^{N_g} C(S'', S''_{\text{int}})/\Theta_i, \quad (5)$$

where  $S''$  and  $S''_{\text{int}}$  are defined as

$$S'' = S^j (M_{\text{HI}}^i/M_{\text{HI}}^j) (W^j/W^i), \quad (6)$$

$$S''_{\text{int}} = S^j_{\text{int}} M_{\text{HI}}^i/M_{\text{HI}}^j. \quad (7)$$

Stable solutions for  $V_{\text{eff}}^i$  are found after  $\sim 25$  iterations. These values of  $V_{\text{eff}}^i$  are found for each galaxy individually and are the maximum likelihood equivalents of  $V_{\text{max}}$  for the standard  $\Sigma 1/V_{\text{max}}$  method (Schmidt 1968). Summing the values of  $1/V_{\text{eff}}^i$  in bins of H I mass gives the original 2DSWML solution for the H I mass function. However, for maximum likelihood estimators of the space density of objects, the normalisation is lost and has to be determined afterwards. This is done by calculating the mean galaxy density  $\bar{n}$  via the minimum variance estimator (Davis & Huchra 1982) and setting  $\bar{n}$  equal to the integral over the H I mass function. To take into account the effects of sample variance on galaxy density, the selection function is weighted by the inverse of the second moment of the two-point correlation function, which is set to  $J_3 = 8000 h_{75}^{-3}$  Mpc $^3$  (Meyer et al. 2005). The selection function  $S$  is calculated similarly as in Z03. Only the distance range corresponding to  $0.001 < S < 0.1$  is used in the calculation of  $\bar{n}$ , to avoid adding noise from the farthest and nearest regions of velocity space where the number of galaxies is low. After this normalisation is applied to  $V_{\text{eff}}^i$ , these values represent true volumes. The method was tested extensively using synthetic samples, similar to what is described in Z03.

## 3 RESULTS

In principle, the 2DSWML technique can be applied to the full HICAT sample, including the detections for which the expected completeness is very low. However, including the detections for which  $C \ll 1$  implies large corrections to the expected space densities (see Eq.5). To avoid this, we choose to cut the sample at  $C > 0.5$ . This reduces the total sample by only 7% to 4010. For the completeness function  $C$  we adopt the parametric approximation based on an error function calculated in Zwaan et al. (2004), and to account for the varying noise level across the sky, we adopt the completeness correction suggested in that paper. We note that the latter correction has an insignificant effect on the HIMF. In Zwaan et al. (2004) we found that HICAT is complete at the 95%

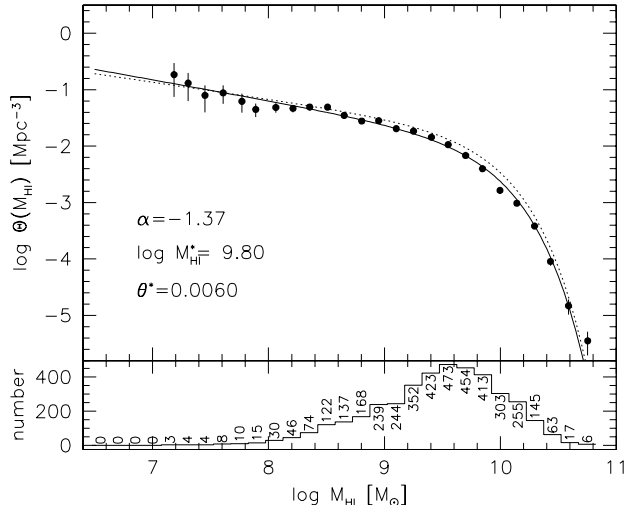


**Figure 1.** Top: H I mass function from HICAT. The solid line is a Schechter fit to the points, the best-fit parameters are shown in the lower left corner; Bottom: Distribution of H I masses used for the HIMF calculation.

(99%) level at a peak flux of 68 (84) mJy and at an integrated flux of 7.4 (9.4) Jy km s<sup>-1</sup>

Figure 1 shows the result of the analysis. The top panel shows the HIMF, the bottom panel shows a histogram of the number of galaxies in each H I mass bin. The errors on the HIMF points are from Poisson statistics. A Schechter function defined by

$$\Theta(M_{\text{HI}})dM_{\text{HI}} = \theta^* \left( \frac{M_{\text{HI}}}{M_{\text{HI}}^*} \right)^\alpha \exp \left( -\frac{M_{\text{HI}}}{M_{\text{HI}}^*} \right) d \left( \frac{M_{\text{HI}}}{M_{\text{HI}}^*} \right), \quad (8)$$

is fitted to the points and shown by a solid line. The parameters of this fit are:  $\alpha = -1.37 \pm 0.03$ ,  $\log(M_{\text{HI}}^*/M_{\odot}) = 9.80 \pm 0.03 h_{75}^{-2}$ , and  $\theta^* = (6.0 \pm 0.8) \times 10^{-3} h_{75}^3 \text{ Mpc}^{-3}$ . The uncertainties on the Schechter parameters are determined by jackknife resampling (Lupton 1993), where the sky is divided into 24 equal area regions. This jackknife resampling procedure includes the uncertainties due to large-scale structure and possible errors due to the varying noise level across the sky. The dimensionless covariance between  $\alpha$  and  $\log M_{\text{HI}}^*$  is  $r(\alpha, \log M_{\text{HI}}^*) = -0.53$ , indicating the strong correlation between these two parameters, as is normally seen in galaxy luminosity and mass function fits. We note that  $\log M_{\text{HI}}^*$  and  $\theta^*$  are also highly covariant:  $r(\log M_{\text{HI}}^*, \theta^*) = -0.83$ , which illustrates that quoting values of  $\log M_{\text{HI}}^*$  or  $\theta^*$  individually is not very meaningful: the combination of these two parameters defines  $\Omega_{\text{HI}}$ . For completeness, we note that  $r(\alpha, \theta^*) = 0.32$ .

For comparison, the HIMF derived from the BGC (Z03) is plotted as a dashed curve. The new HICAT HIMF is slightly steeper than the Z03 HIMF, for which we found  $\alpha = -1.30 \pm 0.08$ , but within the errors. The new measurement is also in reasonable agreement with previous HIMF measurements from blind 21-cm surveys, which showed values of  $\alpha = -1.2$  (Zwaan et al. 1997),  $\alpha = -1.52$  (Kilborn 2000),  $\alpha = -1.51$  (Henning et al. 2000), and  $\alpha = -1.53$  (Rosenberg & Schneider 2002). We refer the reader to Z03 for a complete discussion of previous HIMF measurements from blind 21-cm surveys.

In Figure 2 we show the redshift distribution of the HICAT sample. A good method to test the validity of the method used to calculate the HIMF is to compare this distribution with the predicted distribution from the derived selection function  $S$ . This predicted distribution is shown by the dashed line, which appears to be

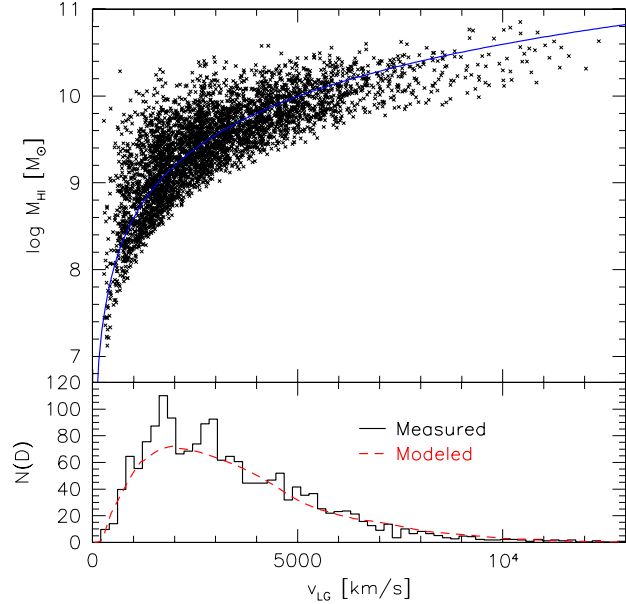


**Figure 2.** Top: H I masses of HICAT detections as a function of their redshift. Points above the solid line are integrated flux-limited at  $S_{\text{int}} = 9.4 \text{ Jy km s}^{-1}$  (Zwaan et al. 2004). Only points that are used in the HIMF calculation ( $C > 0.5$ ) are shown. Bottom: Redshift distribution of HICAT galaxies. The histogram shows the measured distribution and the dashed line is predicted distribution based on the selection function calculated from the maximum likelihood method.

an excellent approximation to the real HICAT selection. Similarly to what we found in Z03, the number counts predicted from the selection function ( $0.174 \text{ deg}^{-2}$ ) is only 7% lower than the measured number counts ( $0.186 \text{ deg}^{-2}$ ). This difference is due to the two over-densities seen at  $\sim 1500$  and  $\sim 2500 \text{ km s}^{-1}$ .

### 3.1 Biases in the HIMF determination

In Z03 we discussed in detail the various biases in the determination of the HIMF based on the Bright Galaxy Catalogue. It was found that the selection bias and H I self-absorption have the strongest effects on the HIMF and  $\Omega_{\text{HI}}$ . For brevity, we choose not to repeat here all the tests of biases in the determination of the HIMF, but only briefly discuss the ones that may be particularly relevant to HICAT and refer the reader to Z03 for a detailed description of biases.

*Selection bias* — The selection bias is the effect that noise on detection spectra preferentially causes peak fluxes to be overestimated, which may result in an increased number of low-flux detections in the sample. Similarly to Z03, we simulate this effect and find that due to the selection bias the global space density of objects is probably overestimated by  $\approx 10\%$ , and the slope of the HIMF becomes steeper by  $\approx -0.05$ . Together, this causes an overestimation of  $\Omega_{\text{HI}}$  of  $\approx 15\%$ .

*H I self absorption* — The effect of H I self-absorption is very difficult to assess from the HIPASS data. We conservatively adopt the result from Zwaan et al. (1997) that H I self-absorption causes a small decline in the measured space density and the knee of the HIMF, resulting in underestimation of the measured  $\Omega_{\text{HI}}$  of  $\leq 15\%$ .

*Deviations from Hubble flow* — Masters, Haynes, & Giovanelli (2004) recently argued that calculating distances to galaxies by assuming a pure Hubble flow

instead taking into account the local velocity field, can lead to errors in the slope of the HIMF. We test this by adopting the Mould et al. (2000) distance model and recalculate the HIMF. The low-mass slope of this HIMF is  $\alpha = -1.39 \pm 0.03$  not significantly different from our HIMF based on pure Hubble flow distances in the Local Group reference frame. Masters et al. (2004) concluded that the Z03 HIMF slope was probably underestimated and they suggest a slope of  $\alpha = -1.4 \pm 0.1$ , which is in excellent agreement with our new HICAT slope. The median distance of the HICAT sample is larger than that of the Z03 sample, which implies that the fractional distance errors due to peculiar motions are smaller. This explains why taking into account the local peculiar velocity field does not have a significant effect on the HICAT HIMF slope.

*Lower distance limit* — To avoid confusion with Galactic high-velocity clouds (HVCs), we applied a lower limit of  $v_{\text{gsr}} < 300 \text{ km s}^{-1}$  to HICAT. Obviously, this constraint also excludes very nearby, low mass galaxies from the present analysis. Our previous HIMF determination based on the Bright Galaxy Catalogue (Z03) had a measurement at  $M_{\text{HI}} = 10^{6.8} M_{\odot}$ , but the lowest H I mass point for HICAT is at  $M_{\text{HI}} = 10^{7.2} M_{\odot}$ . In Z03 we argued that for peak-flux-limited samples, imposing a lower distance limit can cause a slight drop of the HIMF at very low H I masses. For HICAT we find that this effect is not measurable because the sample is not strictly peak-flux-limited.

#### 4 ENVIRONMENTAL EFFECTS ON THE HIMF

Rosenberg & Schneider (2002) speculated on the effects of environment on the slope of the HIMF. They concluded that the HIMF in the immediate region around the Virgo cluster was  $\alpha \approx -1.2$ , flatter than in the field region where they found  $\alpha \approx -1.5$ . Our sample of HICAT galaxies is sufficiently large to test the effect of local density on the shape of the HIMF, by subdividing the catalogue into samples drawn from different local densities.

We choose to parameterise local density by calculating the distance  $r_n$  to the  $n$ -th nearest neighbour for all HICAT galaxies. Densities are calculated as  $\rho_n = n/[(4/3)\pi r_n^3]$ , and normalised to the median density to obtain  $\rho_n / \langle \rho_n \rangle$ . We divide the HICAT sample into five logarithmically spaced subsamples with different mean densities. Since HICAT is increasingly sparsely sampled at larger redshift, nearest neighbour measurements increase rapidly as a function of redshift. Therefore, different subsamples could effectively be drawn from different redshift ranges. This, in turn, implies preferential selection of certain H I mass ranges for each subsample (see Fig. 2), which could bias the HIMF calculation. We correct for this effect by first fitting a power-law to the conditional probability distribution of nearest neighbour distance as a function of redshift. Next we subtract this power-law fit from the nearest neighbour distances to obtain an unbiased nearest neighbour measurement of which, however, the absolute calibration is now lost. We test that our corrected nearest neighbour measurements sample all distances equally by calculating for each subsample the mean and the dispersion of the redshifts. We confirm that there are no significant differences in the redshift distributions of the subsamples. Finally, to prevent including galaxies from the most sparsely sampled redshift range, we limit our calculations to galaxies with  $v_{\text{gsr}} < 5000 \text{ km s}^{-1}$ .

The HIMF as a function of local density  $\rho_5 / \langle \rho_5 \rangle$  is shown in Fig. 3. We find evidence for a weak dependence of the HIMF slope on density environment, in the sense that the low-mass end of

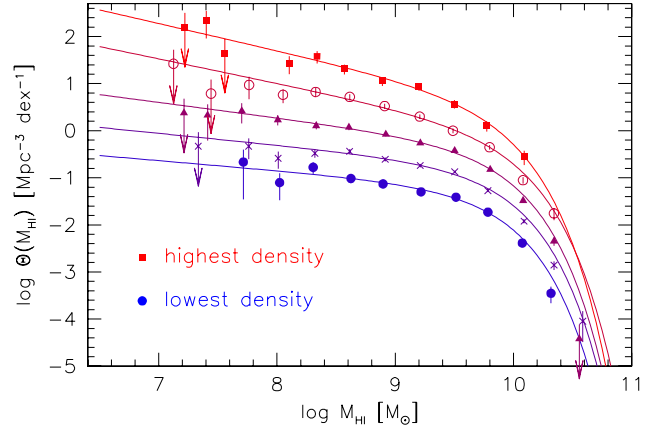


**Figure 3.** The H I mass function as a function of local galaxy density. The HICAT sample has been divided into five logarithmically spaced subsamples according to the density out to the fifth nearest neighbour. The HIMF for each subsample is shown with the corresponding best fit Schechter function. The HIMFs are offset from each other vertically by 0.5 dex.

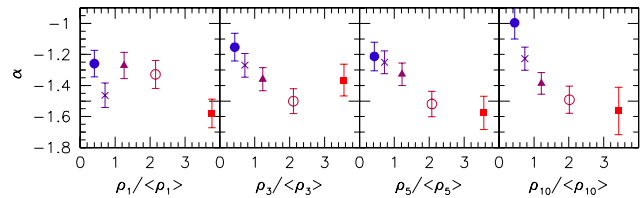


**Figure 4.** The low-mass slope  $\alpha$  of the Schechter function fits to the H I mass function as a function of local galaxy density. The different panels show the results based on the first, third, fifth, and tenth nearest neighbour, from left to right.

the HIMF becomes *steeper in higher density regions*. There is no corresponding correlation between the density and the characteristic mass  $M_{\text{HI}}^*$ . In addition to this analysis based on the fifth nearest neighbour, we also calculated densities on smaller and larger scales, out to the first, third, and tenth nearest neighbour, respectively. The results based on these measurements are shown in Figure 4, where the Schechter low-mass slope  $\alpha$  is plotted as a function of density. Interestingly, the effect of steeper HIMFs toward higher density regions appears to become stronger toward larger scales, indicating that the environmental effects on the H I properties of galaxies are not restricted to short distance effects such as galaxy interactions, but also operate on larger scales.

Our observed trend between the slope of HIMF low-mass end with density is in qualitative agreement with Croton et al. (2004), who use the 2dF galaxy redshift survey to show that the slope of the luminosity function is weakly dependent on environment. Our results cannot be quantitatively compared to those of Croton et al. (2004) because we use a different method to parametrise local density. Furthermore, our density measurements are based on H I-selected galaxies only, while Croton et al. (2004) use optically selected galaxies. It should also be kept in mind that the dynamic range in densities probed by HIPASS is smaller than that probed by optical surveys. For example, Waugh et al. (2002) showed that cluster centres that are readily apparent in the counts of optical galaxies are only detected as over-densities of a few times the density of H I-detected galaxies in the field. At first sight, our findings seem to be in conflict with the recent results of Springob et al. (2004), who, based on optically selected galaxies, claim a flattening of the HIMF

toward higher density regions. However, the statistical significance of their result is low and the HIMFs from the highest and lowest density subsamples are consistent at the  $1\sigma$  level.

Interestingly, recent 2dF and SDSS results show an anti-correlation between star formation rates based on the equivalent width of the H $\alpha$  emission line and galaxy density (Lewis et al. 2002; Gómez et al. 2003; Balogh et al. 2004), out to large distances from cluster cores. Kauffmann et al. (2004) and Tanaka et al. (2004) also find that the specific star formation rate  $SFR/M_*$ , is strongly dependent on environment, but furthermore conclude that this relation is most pronounced for the lower mass galaxies. This implies that the comparative rate at which lower mass galaxies consume their innate HI gas with respect to higher mass galaxies is greater in low density environments than high density environments. Hence, this effect leads to a flattening of the HIMF in low density regions. Of course, this is a simplified view of galaxy evolution because it is well established that gas accretion plays an important role in the total neutral gas budget of galaxies (e.g., Matteucci & Francois 1989), but it can go a long way in explaining our observed correlation between HIMF slope and density.

An alternative explanation can be found in the halo-occupation model in which galaxy properties depend solely on dark matter halo mass, which is predicted by the cold dark matter (CDM) theory. Mo et al. (2004) predict that in this model the shape of the luminosity function of late type galaxies is independent of local density because these galaxies live in low-mass halos. Early type galaxies mainly exist in high-mass halos, which are associated with higher density regions. It is known that the HI masses of early type galaxies are typically low, and their HIMF is steeper than that of late type galaxies (Zwaan et al. 2003). Therefore, a relatively higher contribution of lower HI masses (and hence a steeper HIMF) in higher density regions is a direct prediction of the CDM model.

## 5 CONCLUSIONS

In Z03 we presented the HI mass function of galaxies based on the 1000 HIPASS galaxies with the highest peak fluxes. That paper gives a detailed description of the HIMF calculation, the possible effects that may bias the calculation, and discussed the results. This *Letter* presents an updated HIMF measurement from the full HIPASS sample. We find  $\alpha = -1.37 \pm 0.03 \pm 0.05$ ,  $\log(M_{\text{HI}}^*/M_{\odot}) = 9.80 \pm 0.03 \pm 0.03 h_{75}^{-2}$ , and  $\theta^* = (6.0 \pm 0.8 \pm 0.6) \times 10^{-3} h_{75}^3 \text{ Mpc}^{-3}$  (random and systematic uncertainties at 68% confidence), in good agreement with the Z03 results. The slope of the HIMF is comparable to that of the optical luminosity function from the SDSS measured down to low absolute magnitudes of  $M_r \sim -13$  (Blanton et al. 2004).

We find tentative evidence for a steepening of the low-mass end of the HIMF as a function of local galaxy density. This effect becomes stronger if local densities are measured over larger scales, which indicates that environmental effects on the HI properties of galaxies are not restricted to short distance effects such as galaxy interactions.

HIPASS is a relatively shallow survey compared to some of the small area deep surveys. However, because of the large sky coverage the number of detections is very large and the HIMF can be measured with high accuracy. HIPASS has particularly good statistics at the high mass end of the HIMF, which dominates the mass density of neutral hydrogen. Therefore,  $\Omega_{\text{HI}}$  is measured with high accuracy:  $\Omega_{\text{HI}} = (3.5 \pm 0.4 \pm 0.4) \times 10^{-4} h_{75}^{-1}$ .

The faint-end tail of the HIMF is measured well down to HI masses of  $10^{7.2} M_{\odot}$ . No other survey has been able to constrain the HIMF better at this mass limit. The space density of objects much below  $M_{\text{HI}} = 10^7 M_{\odot}$  is still not accurately known. A number of surveys have been able to put upper limits on the space density of these low HI mass systems in higher density regions (e.g., de Blok et al. 2002; Zwaan 2001), but large scale ‘blind’ surveys with existing technology are probably not able to make significantly better measurements in this region of parameter space. Future large radio telescopes are required to measure reliably the space density of objects much below  $M_{\text{HI}} < 10^7 M_{\odot}$ .

## REFERENCES

- Balogh M., et al., 2004, MNRAS, 348, 1355
- Blanton M. R., et al., 2001, AJ, 121, 2358
- Blanton M. R., Lupton R. H., Schlegel D. J., Strauss M. A., Brinkmann J., Fukugita M., Loveday J., 2004, astro-ph/0410164
- Briggs F. H., 1990, AJ, 100, 999
- Cross N., Driver S. P., 2002, MNRAS, 329, 579
- Croton D. J., et al., 2004, astro-ph/0407537
- Davis M., Huchra J., 1982, ApJ, 254, 437
- de Blok W. J. G., Zwaan M. A., Dijkstra M., Briggs F. H., Freeman K. C., 2002, A&A, 382, 43
- Driver, S., et al., 2005, MNRAS, submitted
- Disney M. J., 1976, Nature, 263, 573
- Efstathiou G., Ellis R. S., Peterson B. A., 1988, MNRAS, 232, 431
- Gómez P. L., et al., 2003, ApJ, 584, 210
- Henning P. A., et al. 2000, AJ, 119, 2686
- Hogg D. W., et al., 2003, ApJ, 585, L5
- Kauffmann G., White S. D. M., Heckman T. M., Ménard B., Brinchmann J., Charlot S., Tremonti C., Brinkmann J., 2004, MNRAS, 353, 713
- Kilborn V. A., 2000, PhD thesis, The University of Melbourne
- Koribalski B., et al., 2004, AJ, in press
- Kraan-Korteweg R. C., van Driel W., Briggs F., Binggeli B., Mostefoui T. I., 1999, A&AS, 135, 255
- Lewis I., et al., 2002, MNRAS, 334, 673
- Lupton, R. 1993, Statistics in Theory and Practise (Princeton: Princeton Univ. Press)
- Masters K. L., Haynes M. P., Giovanelli R., 2004, ApJ, 607, L115
- Matteucci, F. & Francois, P. 1989, MNRAS, 239, 885
- Meyer M. J., et al., 2004, MNRAS, 350, 1195
- Meyer M. J., Zwaan, M. A., Webster, R. L., Brown, M., Staveley-Smith, L., 2005, in preparation
- Mo H. J., Yang X., van den Bosch F. C., Jing Y. P., 2004, MNRAS, 349, 205
- Mould J. R., et al., 2000, ApJ, 529, 786
- Péroux, C., McMahon, R. G., Storrie-Lombardi, L. J., & Irwin, M. J. 2003, MNRAS, 346, 1103
- Rosenberg J. L., Schneider S. E., 2002, ApJ, 567, 247
- Schneider S. E., Spitzak J. G., Rosenberg J. L., 1998, ApJ, 507, L9
- Schmidt M., 1968, ApJ, 151, 393
- Springob, C. M., Haynes, M. P., Giovanelli R., 2004, astro-ph/0411349
- Storrie-Lombardi, L. J. & Wolfe, A. M. 2000, ApJ, 543, 552
- Tanaka M., Goto T., Okamura S., Shimasaku K., Brinkmann J., 2004, AJ, 128, 2677
- Waugh M., et al., 2002, MNRAS, 337, 641
- Zwaan M. A., Briggs F. H., Sprayberry D., Sorar E., 1997, ApJ, 490, 173
- Zwaan M. A., 2001, MNRAS, 325, 1142
- Zwaan M. A., et al., 2003, AJ, 125, 2842 (Z03)
- Zwaan M. A., et al., 2004, MNRAS, 350, 1210